ROTATION AND INCIDENCE ANGLES FOR PARABOLIC TROUGH

M.M. El-Kassaby
Mechanical Engineering Department, Faculty of Engineering,
Alexandria University, Alexandria, Egypt.

ABSTRACT

A descriptive geometry method is utilized to derive the rotation angles and the incidence angles for a parabolic trough at different orientations. Using least squares method, a system of empirical equations were developed for calculating the solar radiation for Alexandria city, Egypt. A comparison between the empirical correlation and experimental measured data shows a good agreement. Another comparison between the obtained rotation and incidence angles with their corresponding available correlation shows an excellent agreement. The presented equations give the general equations specially for N-S trough tilted with any tilt angle β.

INTRODUCTION

The interest in concentrating collector began to develop when it was realized that flat-plat devices could not meet many thermal needs [1]. Perhaps the most common linear focus device is the parabolic cylinder concentrator " parabolic trough" [2-5]. Efficiencies of these collectors are in the neighborhood of 60 to 70 % when operating at about 150 °C above ambient at near normal incidence [6].

The parabolic trough is usually oriented east-west horizontal, north south horizontal, or north-south and parallel to the earth's axis of rotation (polar axis [6]), in which the reflector tracks the solar azimuth angles around the axis [1,7]. A review of technology and thermal performance of intermediate temperature solar collector was given by Wyman et al[8].

Many investigators have studied the performance of the parabolic collector and the effect of focal length error on the parabolic performance [9,10 and 11]. A design of sun tracker was described by Lynch and Salamah [12]. In their design two electro-optic sensors and a small low-cost electronic control circuit were used.

A Curex corporation [13] designed a parabolic trough of a single-axis tracking type. In their tracking electronics controls, three separate modes of operation were conducted; normal tracking, desteer, and stow. Normal tracking would occur when the sun is out and the wind is acceptably low for normal solar system functioning. Desteer is used to direct the collector slightly off-focus to temporarily reduce fluid heating for system control and to avoid fluid over temperature damage in the event of loss of fluid recirculation. In the stow mode, the collector is rotated to a near-inverted position to avoid storm damage and to reduce cleaning procedures.

To the knowledge of the author, no general equations for both rotation and incidence angle are given for both N-S, horizontal and N-S tilted with an angle β. This was the aim of the present work, which could be of a great help in designing a tracking mechanism and in optimizing system design.

THEORETICAL ANALYSIS

To simulate the sun motion over any day, the following system of equations are adopted. The declination angle δ, can be found from equation of Cooper [14].

$$\delta = 23.45 \sin\left(360 \frac{284+n}{365} \right) \quad (1)$$

The incidence angle i, on the horizontal surface was taken as given in [15].

$$\cos i = \sin\delta \sin L + \cos\delta \cos L \cos h_{sr} = \sin\alpha \quad (2)$$

For parabolic trough, the instantaneous incidence angle, tilt angle, rotation angle and shadow angle can be analyzed for each orientation as follows:

a) E-W with daily adjustment

The incidence angle can be found as given in [15].

$$\cos i = \sin\beta \sin\delta + \cos\beta \cos\delta \cos h_{sr} \quad (3)$$

where β is the optimum tilt angle for the required day as given in [16]

$$\beta = \beta_{opt} = L - \tan^{-1}\left[\frac{h_{ss}}{\sin h_{ss}} \tan(\delta)\right] \quad (4)$$

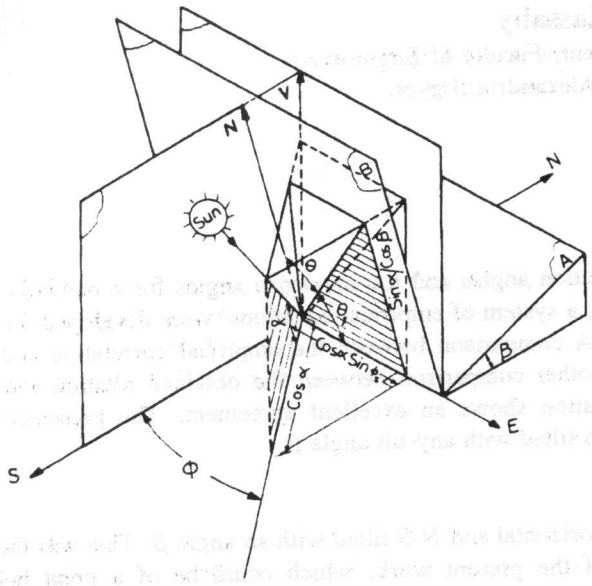

Figure 1. Shadow angle θ for parabolic trough oriented E-W with a fixed tilt angle β.

In Figure (1), the aperture plane is plane A, and the normal plane containing the focus line is plane B. The shadow angle θ, defined as the angle between the normal to the aperture reflector surface and the projection of the sun rays in the focal plan, can be derived from the geometry as:

$$\theta = 90 - \tan^{-1} \frac{\sin \alpha}{\cos \beta \cos \alpha \sin \phi} \quad (5)$$

b) E-W with continuous adjustment

In Figure (2), the aperture plane for the reflector is denoted by plane A. The focal plane will be plane B. If plane A is tilted with an angle equal to β, such that it contains the sun,s rays, plane A will be in a new position say A′. Consequently plane B will be in a new position B′. Plane C is the perpendicular plane for both A and B. From the figure, it is easy to prove that the instantaneous tilt angle β can be given as:

$$\beta = \tan^{-1} \{\cos \phi / \tan \alpha\} \quad (6)$$

and the shadow angle θ, which is also the incidence angle, can be given as:

$$\theta = \text{Sin}^{-1} \{\text{Cos } \alpha \text{ Sin } \phi\} \quad (7)$$

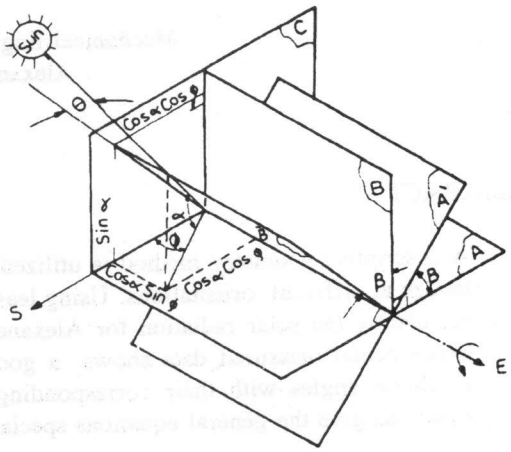

Figure 2. Tilt angle β and shadow angle θ for parabolic trough oriented to E-W horizontal.

c) N-S horizontal

When this orientation is used, tracking is accomplished by rotation of the trough about the long axis of the trough by 180°C in a day. In Figure (3), the aperture surface of the reflector is presented by plane A. plane B is the focal plane and plane C is the perpendicular for both A and B. If plane A rotates by an angle γ such that the sun rays are parallel to plane B, the new positions of planes A and B will be A′ and B′ respectively. In this case γ represents the instantaneous rotation angle. From the figure, it is easy to prove that

$$\gamma = \tan^{-1} \{\text{Sin } \phi / \tan \alpha\} \quad (8)$$

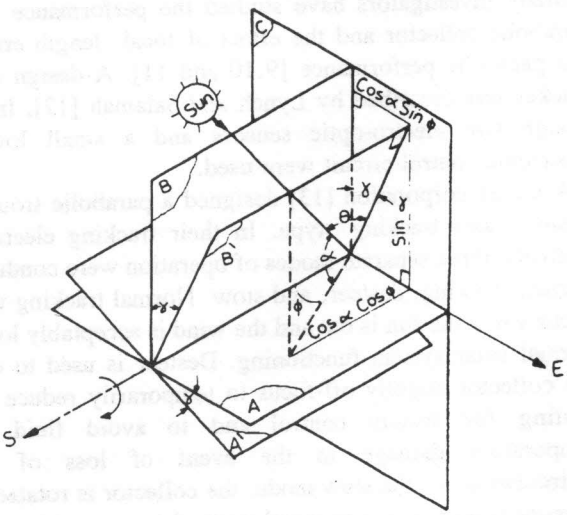

Figure 3. Rotation angle γ, shadow angle θ for parabolic trough oriented to N-S horizontal.

d) N-S orientation, Polar mount

The tilt angle is a very important parameter for N-S parabolic trough. A reasonable compromise for year round operation is to tilt the trough at the latitude angle (β=L). In such orientation, the shadow angle θ is equal to solar declination angle δ at noon time [6,7].

Figure (4) is drawn as an attempt to generalize the solution for the shadow angle (incidence angle) and the rotational angle ω. In the figure, plane A represents the aperture plane for the reflector surface when it is in horizontal position. Plane A becomes A′ when it is tilted with an angle β. It becomes A" when it rotates with an angle ω, such that the sun rays become parallel to the focal plane B′. Plane C represents the perpendicular plane for both A and B. With the aid of the figure, the instantaneous rotation angle ω can be driven. (see appendix A).

$$\cos\omega = \frac{1}{2}\left[\frac{\tan\phi_1}{\tan\beta} + \frac{\tan\beta}{\tan\phi_1} - \frac{1}{\sin\beta\cos\beta\tan\phi_1}\right] - \frac{1}{2}\left[\frac{1}{\tan\beta\sin\phi_1\cos\phi_1} - \frac{2\cos\phi_2}{\sin\beta\sin\phi_1}\right] \quad (10)$$

where angles ϕ_1, ϕ_2 are given in appendix A. Also the shadow angle θ (which is also the incidence angle) is given as

$$\cos\theta = [\cos\alpha\cos\phi\tan\beta + \sin\alpha]\{\sin\phi_3 / \cos\gamma\} \quad (11)$$

The derivation of the previous equations are given in appendix A.

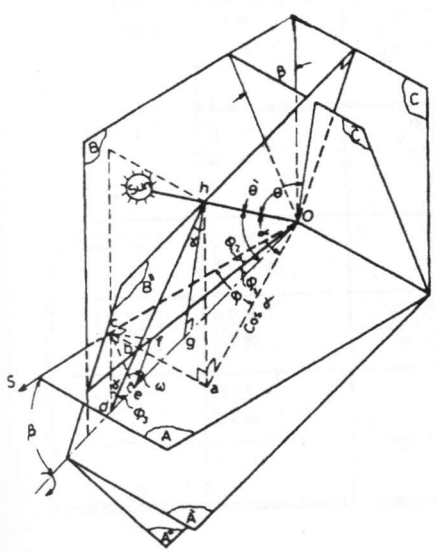

Figure 4. Rotation angle ω and shadow angle θ for N-S orientation, tilt with an angle β.

In all parabolic troughs orientations the shaded length (X) can be found as

$$X = f\tan\theta \quad (12)$$

Also, the instantaneous amount of beam radiation intercepted by the absorber surface (without glass cover) can be found as:

$$I = \rho\,(L_1\text{-}x)\,I_{b,h}[\cos i/\sin\alpha] \quad (13)$$

The monthly mean total hourly solar radiation for Alexandria city recorded in Ref.[17] are taken and a least square method was applied to get empirical correlations for the instantaneous total radiation. The system of equations tabulated in Table 1 is obtained.

RESULTS AND DISCUSSION

The computer results obtained from the empirical equations given in Table 1 are compared with the experimental results given in ref.[17] as shown in Table 2. It can be seen that, the difference between the empirical correlation and the experimental data does not exceed $\pm$ 16 W/m^2 during the summer months and a maximum of $\pm$ 33 W/m^2 for winter time. This differences represent a maximum error of 7.6% of the measured one, which means that the predicted correlations are in a good agreement with the experimental results.

In reference [16], an apparatus consists essentially of a photovoltaic module fixed on a hinged flat plate facing south was used to determine the instantaneous β_{opt} for a given day. Some of these data are used to check the validity of the instantaneous tilt angle β obtained from equation (6). The comparison were tabulated in Table 3. The maximum error between the available experimental data and the computed one was about 2 degree. This difference could be attributed to the difference between the local time and the sun time. Since the experimental data were recorded using the local time, while the calculated data were obtained using the solar time, which is symmetrical around noon time.

Comparison between the present shadow angles (equations 7,9, and 11) and its available corresponding incidence angle are tabulated in Table 3. The incidence angles are given in ref. [15] as:

For E-W continuous adjustment

$$\cos i = \sqrt{1 - \cos^2\delta\,\sin^2 h_{sr}} \quad (14)$$

For N-S horizontal

$$\cos i = \left[(\sin L\sin\delta + \cos L\cos\delta\cos h_{sr})^2 + \cos^2\delta\sin^2 h_{sr}\right]^{\frac{1}{2}} \quad (15)$$

Table 1. Empirical correlations to obtain the average solar radiation for Alexandria region, Egypt (W/m^2).

$M = (N + 15.5) / 30.5$ N = day number	Range M	 t
$I = 0.0$ $I = -270 + 103.5\ M - 5.5\ M^2$ $I = -281.25 + 151.85\ M - 13.25\ M^2$ $I = 0.0$	$M<3$ $3<M\leq6$ $6<M\leq9$ $9<M$	$t<6$ $t=6$ $t=6$ $t=6$
$I = 9.99 - 19.9286\ M + 26.1429\ M^2 - 2.5\ M^3$ $I = -1785 + 794.929\ M - 95.8571\ M^2 - 3.5\ M^3$	$M\leq6$ $M>6$	$6<t\leq7$ $6<t\leq7$
$I = 96.66 + 13.693\ M + 19.504\ M^2 - 2.0463\ M^3$ $I = -1687.67+803.742\ M-95.2262\ M^2+3.389\ M^3$	$M\leq6$ $M>6$	$7<t\leq8$ $7<t\leq8$
$I = 228 - 7.484\ M + 31.523\ M^2 - 3.277\ M^3$ $I = -2104.5 + 1014.44\ M - 119.44\ M^2 + 4.222\ M^3$	$M\leq6$ $M>6$	$8<t\leq9$
$I = 340.33 - 12.665\ M + 36.8\ M^2 - 3.8148\ M^3$ $I = 24305 - 144455.3\ M + 3454.52\ M^2 - 401.206\ M^3$ $+ 22.5966\ M^4 - 0.495833\ M^5$	$M\leq6$ $M>6$	$9<t\leq10$
$I = 414.667 - 3.37431\ M + 36.8849\ M^2 - 3.74074\ M^3$ $I = 31216.5 - 18206.6\ M + 4274.28\ M^2 - 488.559\ M^3$ $+ 27.1307\ M^4 - 0.5875\ M^5$	$M\leq6$ $M>6$	$10<t\leq11$
$I = 438.667 + 12.6336\ M + 34.7554\ M^2 - 3.629\ M^3$ $I = 25535 - 14948.7\ M + 3549.62\ M^2 - 409.606\ M^3$ $+22.9242\ M^4 - 0.5\ M^5$	$M\leq6$ $M>6$	$11<t\leq12$
$I = 400.667 + 7.00664\ M + 35.2063\ M^2 - 3.65741\ M^3$ $I = 22901.3 - 13332.68\ M + 3150.98\ M^2 - 361.614\ M^3$ $+ 20.0795\ M^4 - 0.433333\ M^5$	$M\leq6$ $M>6$	$12<t\leq13$
$I = 354.667 - 30.4497\ M + 42.111\ M^2 - 4.2963\ M^3$ $I = 18880.6 - 11243.6\ M + 2712.09\ M^2 - 361.686\ M^3$ $+ 17.8674\ M^4 - 0.391667\ M^5$	$M\leq6$ $M>6$	$13<t\leq14$
$I = 183.333 - 28.7553\ M + 19.865\ M^2 - 2.17593\ M^3$ $I = 23485.5 - 13750.9\ M + 3227.73\ M^2 - 368.716\ M^3$ $+20.447\ M^4 - 0.441667\ M^5$	$M\leq6$ $M>6$	$14<t\leq15$
$I = 76 + 44.3373\ M + 9.0238\ M^2 - 1.02778\ M^3$ $I = -1667.52+804.48\ M-96.4762\ M^2+3.4722\ M^3$	$M\leq6$ $M>6$	$15<t\leq16$
$I = 3.33332 - 14.0066\ M + 24.0794\ M^2 - 2.34259\ M^3$ $I = -1910.19 + 837.944\ M - 101.238\ M^2 + 3.722\ M^3$	$M\leq6$ $M>6$	$16<t\leq17$
$I = 0.0$ $I = -250 + 95\ M - 5\ M^2$ $I = -229.55 + 132.15\ M - 11.75\ M^2$ $I = 0.0$	$M\leq6$ $M>6$	$t>17$

Table 2. Monthly mean total hourly radiation for Alexandria, Egypt (W/m^2).

Mon,	Time												
	6	7	8	9	10	11	12	13	14	15	16	17	18
*	00	13	127	237	362	446	480	440	364	230	119	10	00
J +	00	13	127	248	360	444	483	439	363	229	119	11	00
D	00	00	000	11	-2	-2	3	-1	-1	1	000	1	00
*	00	52	188	310	426	520	547	523	420	301	180	45	00
F +	00	53	185	311	430	523	571	524	426	301	183	52	00
D	00	1	3	1	4	3	24	1	6	000	3	7	00
*	00	120	257	400	540	642	703	645	538	395	256	117	00
M +	00	115	258	397	527	631	689	635	522	386	252	113	00
D	00	-5	1	-3	-13	-11	-14	-10	-16	-9	4	-4	00
*	56	182	330	478	627	750	804	754	624	470	320	174	50
A +	53	185	329	488	629	746	809	752	626	472	321	180	47
D	-3	3	-1	10	2	-4	5	-2	2	2	1	6	-3
*	110	257	400	562	723	851	912	860	720	556	385	250	100
M +	106	248	395	564	718	846	909	853	716	547	382	246	97
D	-4	-9	-5	2	-5	-5	-3	-7	-4	-9	-3	-4	-3
*	153	290	438	612	765	915	976	920	760	600	435	278	140
J +	150	289	4380	608	765	911	974	917	760	586	433	278	137
D	-3	-1	00	-4	000	-4	-2	-3	000	-14	-2	000	-3
*	132	284	436	600	768	904	970	910	763	592	430	270	122
J +	135	285	437	595	767	902	970	897	763	589	430	274	123
D	3	1	1	-5	-1	-2	000	-13	000	-3	000	4	1
*	86	256	384	552	720	845	913	840	708	540	372	216	74
A +	92	239	389	538	731	861	926	813	722	556	379	227	82
D	6	13	5	-14	11	16	13	-27	14	16	7	11	5
*	12	163	300	475	616	737	800	740	610	464	287	153	9
S +	23	166	314	442	629	746	813	712	620	467	300	154	18
D	-11	3	14	-33	13	13	13	-28	10	000	13	1	9
*	00	78	217	336	478	562	643	560	470	328	200	64	00
O +	00	89	228	333	499	597	667	542	493	352	214	78	00
D	00	11	11	-3	21	35	24	-18	23	24	14	14	00
*	00	16	143	264	382	466	528	479	375	257	134	10	00
N +	00	26	152	235	394	477	542	434	386	263	139	18	00
D	00	10	9	-29	12	11	20	-33	11	6	5	8	00
*	00	0	100	221	312	397	438	394	304	214	92	0	00
D +	00	1	104	191	325	408	453	364	316	220	96	3	00
D	00	1	4	-30	13	11	15	-30	12	6	4	3	00

* Experimental data [17]
+ present equation
D difference

Table 3. A comparison between the present obtained equations and the corresponding available data. Also the values for rotation angle γ and ω.

	E-W continuous adjustment				N-S horizontal			N-S polar		
solar time	β eq. (6)	β Ref. (16)	i eq. (14)	θ eq. (7)	i eq. (15)	θ eq. (9)	γ eq. (8)	i=δ	θ eq. (11)	ω eq. (10)
Date 25/11										
8 AM	69.9		53.42	53.48	34.02	33.95	75.70	21.98	21.92	60.0
8:30	64.5	66	47.36	47.42	37.69	37.63	68.44		21.93	52.5
9:	60.7	61	40.97	41.03	41.18	41.12	60.66		21.93	45.0
9:30	57.9	59	34.36	34.43	44.40	44.34	52.26		21.94	37.5
10:	56.0	57	27.62	27.68	47.26	47.21	43.16		21.95	30.0
10:30	54.6	55	20.78	20.84	49.65	49.61	33.32		21.96	22.5
11:	53.7	54	13.89	13.94	51.46	51.43	22.75		21.96	15.0
11:30	53.2	54	6.95	7.00	52.60	52.58	11.59		21.97	7.5
12:	53.0	53	0.0	0.12	52.98	52.98	0.2		21.98	0.1
Date 1/12										
8:30	65.4	66	47.80	47.15	38.23	38.16	68.86	22.61	22.56	52.5
9:	61.5	64	40.75	40.81	41.73	21.67	61.06		22.57	45.0
9:30	58.7	61	34.19	34.25	44.96	44.91	52.65		22.57	37.5
10:	56.7	58	27.49	27.55	47.84	47.79	43.52		22.58	30.0
10:30	55.3	57	20.69	20.75	50.25	50.21	33.62		22.59	22.5
11:	54.3	56	13.82	13.88	52.07	52.05	22.97		22.60	15.0
11:30	53.8	56	6.92	6.98	53.22	53.21	11.71		22.60	7.5
12:	53.6	55	0.0	0.12	53.61	53.61	0.21		22.61	0.1
Date 1/1										
8:30	65.8	68	46.91	46.98	38.54	38.54	69.11	22.98	22.93	52.5
9:	61.4	64	40.61	40.68	42.05	41.99	61.31		22.93	45.0
9:30	59.1	63	43.08	34.15	45.2	45.23	52.88		22.94	37.5
10:	57.1	60	27.41	27.47	48.18	48.13	43.8		22.95	30.0
10:30	55.6	58	20.63	20.59	50.59	50.55	33.8		22.96	22.5
11:	54.7	56	13.78	13.84	52.43	52.11	32.1		22.96	15.0
11:30	54.2	56	6.9	6.96	53.59	53.57	11.78		22.97	7.5
12:	54.0	55	0.0	0.12	53.98	53.98	0.21		22.98	0.1

For N-S, polar

$$i = \delta \tag{16}$$

From Table 3, it is clear that the present equations are in excellent agreement with the equations given in ref.[15]. More over the present equations look simpler. The values for the rotation angle obtained by equation (10) are compared with their equivalent equation given in ref.[18] as:

$$\omega = \tan^{-1}\left[\frac{\sin\phi}{\cos\phi\sin\beta + \tan\alpha\cos\beta}\right] \tag{17}$$

It was found that identical results were obtained from equations (10) and (17).

To study the effect of the length ratio (L/f) on the solar fraction -(defined as the amount of solar radiation which reaches the absorber tube (provided that the absorber tube has a length equal to the length of the reflector) divided by the total solar radiation, i.e the amount of radiation obtained from equation 13 divided by the amount of radiation obtained from Table 1)- the computer model results obtained for different length ratios were plotted in Figures (5) and (6).

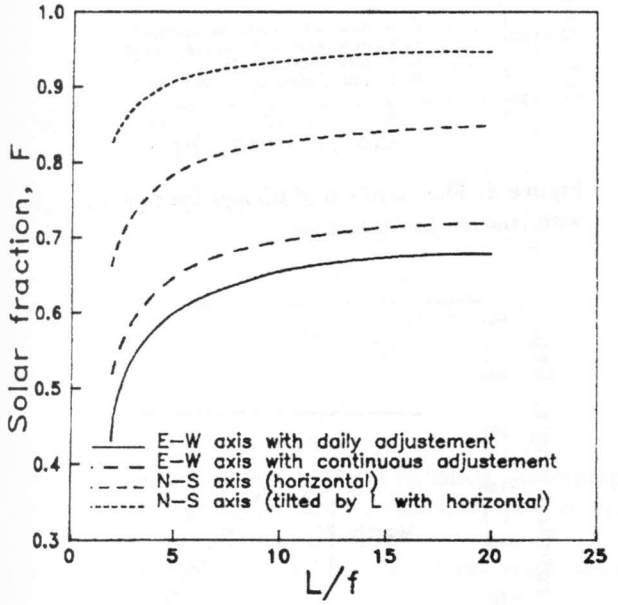

Figure 5. The effect of length ratio (L\f) on the solar fraction F, for a working period equal to the time all over the year.

In Figure (5), the collection period for solar radiation selected to be all the day time, while in Figure (6), that period was selected to be from 8 AM to 16 PM . It is to be noted that the reflectivity of the reflector is taken to be one. That is because it is required to obtain a general solution which does not depend on the optical properties which varies from system to another. It is clear from Figure (5), that the maximum solar fraction is obtained for the N-S, polar parabolic trough. The second is N-S horizontal, with around 10 % less in solar fraction than that for N-S polar one. The E-W with continuous adjustment comes the third. Finally the E-W with daily adjustment had the lowest solar fraction. The figure also shows, as the length ratio increases, the solar fraction increases. The minimum length ratio is suggested to be L/f=5, below which all types of parabolic trough suffer from the shadow effect. The effect of L/f on solar fraction F becomes almost negligible after L/f=10.

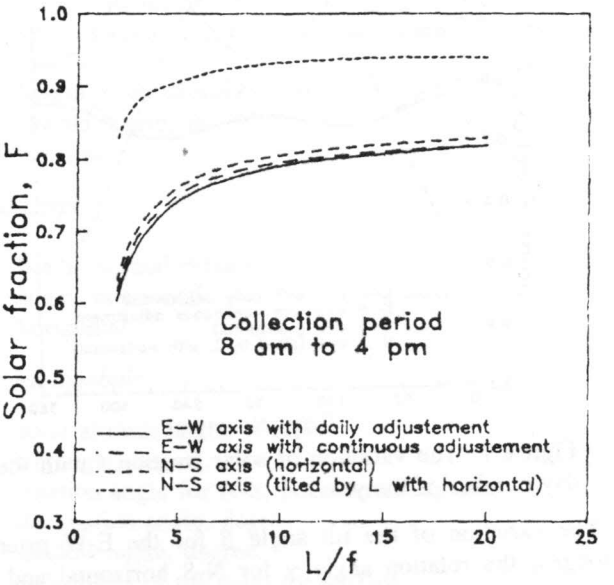

Figure 6. The effect of length ratio (L/f) on the solar fraction F, when the working period is from 8 am to 16 pm all over thee year.

A great improvement in solar fraction F for E-W types is observed when the collecting period becomes only from 8-16 as shown in Figure (6). This is because the shaded length is too large in E-W orientation before 8 AM and after 16 PM, which in turn affects the solar fraction. While the shaded length for N-S orientation is not affected by the day time that much. It is affected mainly by the declination angle.

A comparison for the daily solar fraction F for different parabolic trough orientations, having L/f=5 and a collection period from 8 AM to 16 PM are plotted in Figure (7). It is clear that, the E-W orientation almost gives a constant solar fraction all over the year, but less than that for N-S, orientations. The difference between E-W with daily adjustment and E-W with continuous adjustment is very small and can be ignored (less than 3%). Also the N-S, polar axis gives lower value for solar fraction in summer than its value obtained for N-S horizontal, while it gives higher value during Spring and Autumn. This is because the solar rays at noon approach the N-S, polar trough with an

angle equals to 23.45° in mid summer and -23.45° in mid winter, and are perpendicular in spring and fall. As a result, the solar flux available to the N-S polar trough at solar noon on December 21 and june 21 is cos(23.45) times the solar radiation available at that time. While for N-S horizontal the solar rays are almost perpendicular during the summer time. That is why N-S horizontal performs better than N-S, polar during the summer time. A reasonable compromise is to use a combination of the two types, N-S, polar type for winter, spring and autumn and, N-S horizontal for summer time.

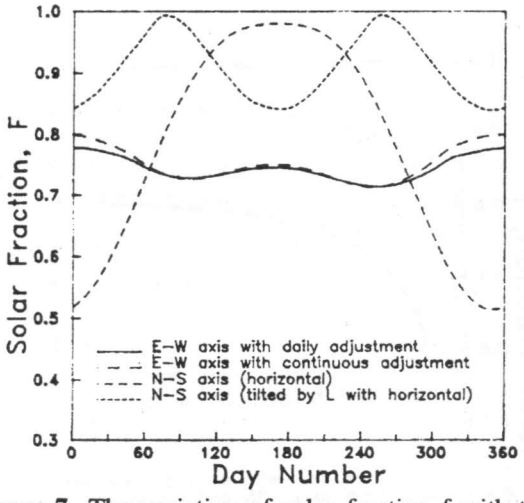

Figure 7. The variation of solar fraction f with the day number of the year.

The variation of the tilt angle β for the E-W oriented troughs, the rotation angle γ for N-S horizontal and the rotation angle ω for N-S, polar mount trough with day time for three selected days are plotted in Figures (8) through (10). The following remarks were observed:

1) for E-W continuous adjustment, the tilt angle increases over that of the fixed angle as the off noon time increase, specially before 8 AM and after 16 PM. this means that the amount collected off the pervious period is almost negligible compared to that through the period itself.
2) The rotation angle for N-S, polar mount, is constant and equal to 15 degree per hour as indicated in Table 3. This value is in excellent agreement with the value given in ref.[17].
3) The difference in β between E-W daily adjustment and E-W continuous adjustment becomes zero at beginning of spring and autumn.
4) The difference between γ and ω becomes very small (less than 2 degree) in March 21 and September 21. Also that difference increases with off noon time increase.
5) For E-W continuous adjustment, the tilt angle β becomes negative in early morning and late afternoon for summer time (June 30), i.e, the collector is facing north. However, the shadow effect is very large in the same period. Therefore no need to bother with that negative angles.

Values of the shaded length X/f versus the solar time for june 30 as a sample day are plotted in Figure (11). The figure shows the shaded length increases rapidly before 8 AM and after 4 Pm for E-W orientation. That is the reason why a great improvement in solar fraction F was found when the collection period was limited to be from 8 AM to 4 PM only.

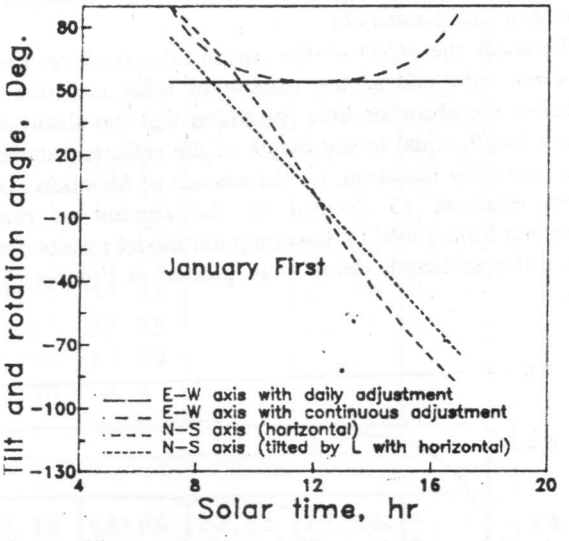

Figure 8. The variation of tilt and the rotation angles with january first day time.

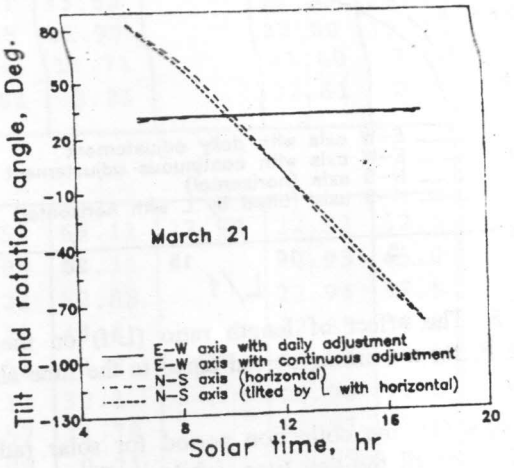

Figure 9. The variation of tilt and the rotation angles with march 21 day time.

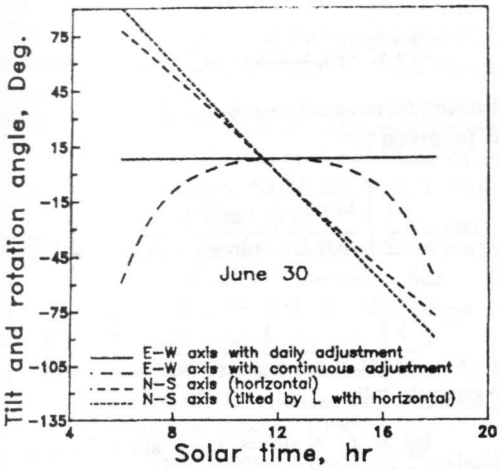

Figure 10. The variation of tilt and the rotation angles with june thirty day time.

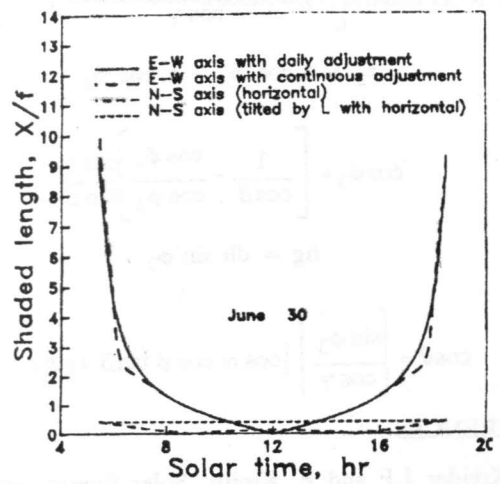

Figure 11. Variation of shaded length ratio (x,f) with june thirty solar time.

CONCLUSION

The following conclusive remarks can be mentioned:

1) The empirical correlation for total radiation concerning Alexandria city given in Table 1 can fairly predict the solar intensity for Alexandria, egypt.
2) The minimum recommended length to focal length ratio is 5.
3) The effect of L_1/f on solar fraction becomes negligible after $L_1/f=10$.
4) To obtain a high value for solar fraction F all over the year, it is recommended to use a combination from N-S horizontal trough during summer time and N-S, polar for the rest of the year.
5) The shaded length (unlighted length) is too large before 8 AM and after 4 PM, specially for E-W orientation.
6) More work is recommended to get the monthly optimum tilt angle for N-S troughs.

ACKNOWLEDGMENT

The author likes to thank Prof. Dr. M.A. Hassab and Dr. A.S. Hegazy for their fruitful advice during performing this work.

NOMENCLATURE

f	focal length,m.
F	Solar fraction.
h_{ss}	the sunrise-hour angle, degree.
h_{sr}	the solar hour angle, degree.
i	incidence angle, degree.
I	solar radiation,W/m^2.
L	latitude angle, degree. Also, the length of the absorber tube,m.
L_1	length of the absorber tube,m.
x	shaded length, m.
t	time, hr

Subscript

b,c	beam, normal surface
b,h	beam, horizontal
h	horizontal

Greek Symbols

α	solar altitude angle, degree.
β	tilt angle, degree.
γ	rotation angle for N-S, horizontal, degree.
δ	declination angle, degree.
θ	shadow angle, degree.
ρ	reflectivity of the collector surface.
ϕ	solar-azimuth angle, degree.
$\acute{\omega}$	rotation angle for N-S, polar, degree.

APPENDIX A

Derivation of the rotation angle for N-S orientation tilted with an angle β.

From Figure (4), different triangles can be drawn as shown in figure A-1, from which the following relations can be derived:

$$x_9 = x_1 \cos \beta \quad \text{(A-1)}$$

$$x_7 = x_1 \sin \beta \quad \text{(A-2)}$$

$$x_2 = \frac{x_1}{\cos \beta} \quad \text{(A-3)}$$

$$x_4 = x_1 \tan \beta \quad \text{(A-4)}$$

$$x = \frac{x_1}{\cos \phi_2} \quad \text{(A-5)}$$

$$x_3 = x_1 \tan \phi_2 = x_4 \tan \gamma \qquad \text{(A-6)}$$

$$x_5 = \frac{x_4}{\cos \gamma} \qquad \text{(A-7)}$$

$$x_6 = x_9 \tan \phi_1 \qquad \text{(A-8)}$$

$$x_{10} = \frac{x_9}{\cos \phi_1} \qquad \text{(A-9)}$$

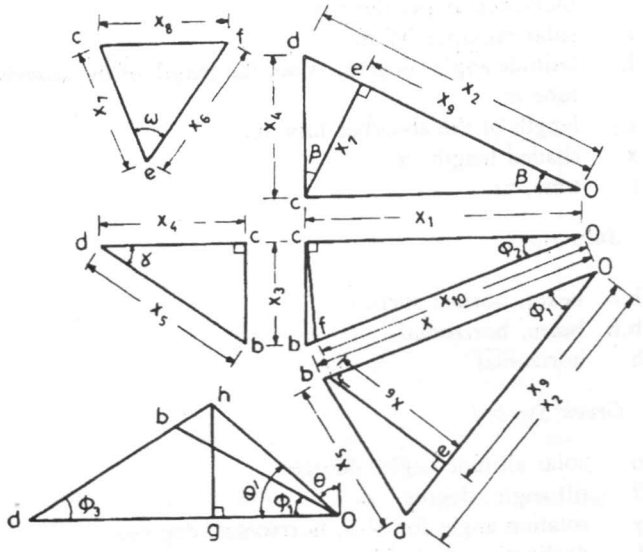

Figure 1.a. Different triangles from Figure 4.

in the plane which contain lines dh,ah

$$ac = ab + bc \qquad \text{(A-10)}$$

If we let the unit length to be represented by the length oh, equation (A-10) can be rewritten as

$$\cos\alpha \sin\phi = \frac{\sin\alpha}{\cos\gamma} \sin\gamma + \cos\alpha \cos\phi \tan\beta \tan\gamma \qquad \text{(A-11)}$$

from which,

$$\tan\gamma = \frac{\cos\alpha \sin\phi}{\sin\alpha + \cos\alpha \cos\phi \tan\beta} \qquad \text{(A-12)}$$

from equation (A-6) the following equation can be derived;

$$\tan \phi_2 = \tan \beta \tan \gamma \qquad \text{(A-13)}$$

from the triangle obd

$$x_5^2 = x^2 + x_2^2 - 2x\, x_2 \cos \phi_1 \qquad \text{(A-14)}$$

from which

$$\cos\phi_1 = \frac{\cos^2\beta \cos^2\gamma + \cos^2\phi_2 \cos^2\gamma - \sin^2\beta \cos^2\phi_2}{2\cos\phi_2 \cos\beta \cos^2\gamma} \qquad \text{(A-15)}$$

from the triangles ocf and ecf

$$x_6^2 + x_7^2 - 2x_6x_7\cos\omega = x_1^2 + x_{10}^2 - 2x_1x_2\cos\phi_2 \qquad \text{(A-16)}$$

substituting from equations A-1,2,8 and 9, the rotation angle ω can be given as:-

$$\cos\omega = \frac{1}{2}\left[\frac{\tan\phi_1}{\tan\beta} + \frac{\tan\beta}{\tan\phi_1} - \frac{1}{\sin\beta\cos\beta\tan\phi_1}\right]$$

$$-\frac{1}{2}\left[\frac{1}{\tan\beta\sin\phi_1\cos\phi_1} - \frac{2\cos\phi_2}{\sin\beta\sin\Phi_1}\right] \qquad \text{(A-17)}$$

in the triangle δdh

$$hd = x_5 + dh = x_5 + \sin\alpha / \cos\gamma \qquad \text{(A-18)}$$

from which

$$hd = \left[\frac{\cos\alpha\cos\phi\tan\beta + \sin\alpha}{\cos\gamma}\right] \qquad \text{(A-19)}$$

$$x_2 = x_5\cos\phi_3 + x\cos\phi_1 \qquad \text{(A-20)}$$

$$\cos\phi_3 = \left[\frac{1}{\cos\beta} - \frac{\cos\phi_1}{\cos\phi_2}\right]\frac{\cos\gamma}{\tan\beta} \qquad \text{(A-21)}$$

$$hg = dh \sin\phi_3 \qquad \text{(A-22)}$$

$$\cos\theta = \left[\frac{\sin\phi_3}{\cos\gamma}\right]\left[\cos\alpha\cos\phi\tan\beta + \sin\alpha\right] \qquad \text{(A-23)}$$

REFERENCES

[1] Kreider J.F and F. Kreith, Solar Energy Handbook, McGraw- hill, chapter 9,1981.

[2] Lof G.O.G and J. A. Duffie, Optimization of Focusing Solar-Collector Design, J. Eng. Power Trans. ASME 85A, 221,1963.

[3] Evans D.L., On the Performance of Cylindrical Parabolic Solar Concentrator with Flat Absorbers, Solar Energy, 19, 379, 1977.

[4] Cobble M. H., Theoretical Concentration for Solar Furnaces, Solar Energy, 5(2), 61, 1961.

[5] Treadwell G. W, Design Consideration for Parabolic Cylindrical Solar Collectors, Sharing the Sun, Joint Solar Conference 2, 235, Winnipeg 1976.

[6] Duffie J. A and W. A. Beckman, Solar Engineering of Thermal Processes, John Wiley & Sons, 1980.

[7] Donald R., Solar Energy, Prentice-hall, 1981.

[8] Wyman C., Castle; J and F. Kreith, A Review of Collector and Energy Storage Technology for Intermediate Temperature Applications, Solar Energy, 24, 517-540, 1980.

[9] Mobarak; A., Morcos; S. M. and Abdel Motelip,

Performance evaluation of parabolic trough Concentrators Under Local Environmental Conditions, ASRE 86, Vol. 1, No. 17, pp. 177- 186, March 23-26, 1986.

[10] El-Haggan A. M., Effect of Adjusting Errors on the Concentration Distribution at Focal Plane of Parabolic Cylinder Concentrator, ASRE 86, Vol. 1, No. 23, pp. 241- 255, March 23-26, 1986.

[11] Ibrahim; S. M. A, The forced Circulation performance of An Electronically Driven Sun Tracking Concentrator, ASRE 86 Vol. 1, No. 19,pp 191-199, March 23-26, 1986, Cairo, Egypt.

[12] Lynch; A. W. and Z. M. Salameh, Simple Electro-optically controlled Dual-axis Sun Tracker, Solar Energy, Vol. 45, pp. 65-69, 1990.

[13] Muller; T.K., The Curex Cylindrical Parabolic Solar Collector, Solar Proceeding of EDRA, Solar Concentrating Collector Conference Technology, Georgia Institute of Technology, Atlanta G. A., Sept., 26-28, 1977.

[14] Cooper; P.I., The Absorption of Solar Radiation in Solar Stills, Solar Energy, 12,3, 1969.

[15] Kreith; F. and J.F. Kreider, Principles of Solar Engineering, McGraw Hill, 1978.

[16] El-Kassaby; M.M., Monthly and Daily Optimum tilt angle for South facing Solar Collector: Theoretical Model, Experimental and Empirical Correlations, Solar & Wind Technology, Vol. 5, No. 6, pp. 589-596, 1988.

[17] Shehata; M. S., Correlation of total and diffuse solar radiation for Alexandria Region, Egypt, M.Sc. Thesis, Alex. University, 1988.

[18] Hassab; M.A, Hegazy; A.S. and M.M. El-kassaby, Thermal Utilization of Solar Energy for Temperature Range Between (100-400°C), First report, Submitted to Academy of Scientific Research and Technology, Cairo, Egypt, 1992.